The relationship between oceanic mesoscale variability and atmospheric convection on 10°N in the eastern tropical Pacific Ocean

J. Thomas Farrar and Robert A. Weller

Woods Hole Oceanographic Institution

Abstract

As part of the Pan American Climate Study (PACS), an air-sea interaction mooring was deployed at 10°N, 125°W in the eastern tropical Pacific for 17 months. There were intraseasonal fluctuations in SST caused by meridional advection by mesoscale motions. Analysis of this signal in the broader spatial and temporal context afforded by satellite altimetry data indicates that this intraseasonal (40 to 100-day period) velocity variability on 10°N can be interpreted as Rossby waves with some Doppler shifting by the mean westward flow. The PACS buoy observations further indicate that there is variability in surface solar radiation coupled to the SST signal of the Rossby wave.

The hypothesis that the SST signals of oceanic Rossby waves and other mesoscale variability may affect atmospheric convection is investigated using satellite measurements of SST, columnar cloud liquid water (CLW), and cloud reflectivity. A statistically significant relationship between SST and these cloud properties is identified within the wavenumber-frequency band of oceanic Rossby waves. Analysis of seven years of data indicates that 10-35% of the variance in the logarithm of CLW at intraseasonal periods and zonal scales on the order of 10° longitude can be ascribed to SST signals driven by oceanic Rossby waves.

Introduction

As part of the Pan-American Climate Studies (PACS) field program, a mooring was deployed at 10°N, 125°W for 17 months, measuring upper-ocean temperature, salinity, and velocity. The buoy also carried a complete surface meteorological package measuring wind velocity, air temperature, incoming short and long wave radiation, humidity, barometric pressure, and precipitation. Air-sea heat fluxes were calulated via bulk formulas (Fairall et al., 1996). The mooring site is within the eastern Pacific warm pool and is near the northernmost climatological location of the Inter-tropical Convergence Zone (ITCZ).

Note the 'meanders' in the SST front. Their zonal scale is about 5° longitude.

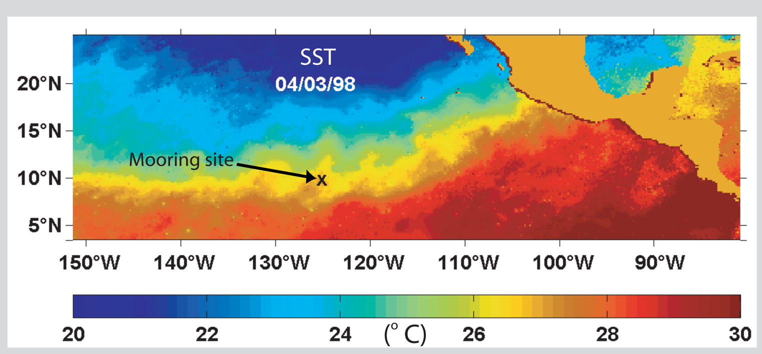

Meridional velocity record from the mooring: The ~60-day velocity fluctuations seen here are responsible for the 'SST meanders' seen above.

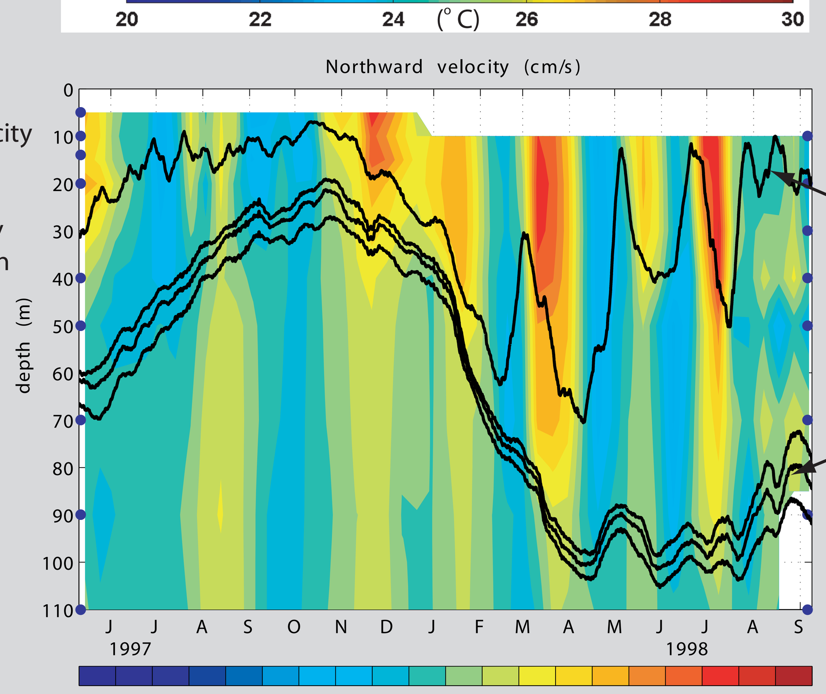

The mooring observations revealed energetic fluctuations in velocity, dynamic height, and SST at a period of about 60 days (see figures above and below). The SST gradient was primarily meridional during the mooring deployment period, as can be seen from satellite SST (above). Comparison of terms in the mixed-layer temperature balance shows that this meridional gradient, together with the strong meridional velocity fluctuations, contributed to a substantial modulation of the local SST at intraseasonal periods during the first half of 1998.

The PACS mooring observations reveal variability in surface heat fluxes that appears coupled to this SST variability. While it is not surprising that there are signals in latent and sensible heat fluxes, the signal in solar heat flux suggests that the mesoscale oceanic variability may modify cloudiness. **The goal of this study is to examine the relationship between mesoscale SST variability on 10°N and cloud properties.**

20-80 day band-pass filtered buoy data.

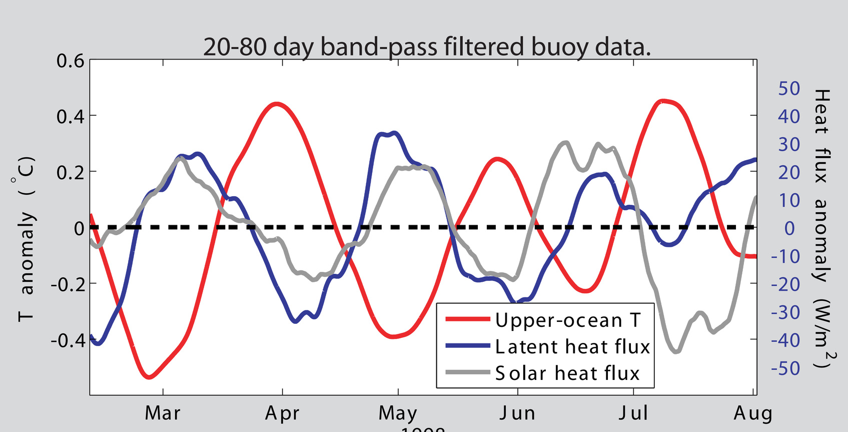

Characteristics of the mesoscale variability and attendant cloud signals

Interpretation of the velocity fluctuations as Rossby waves

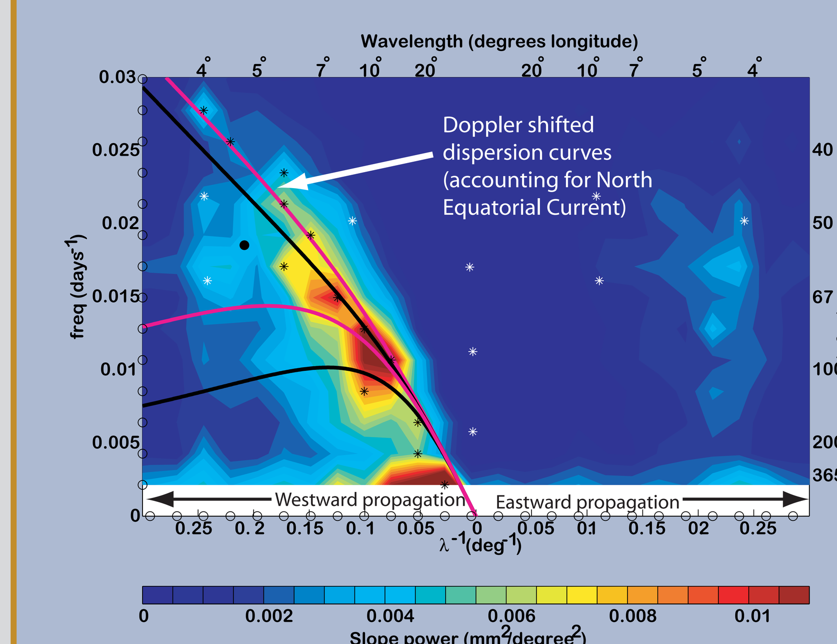

Wavenumber-frequency spectrum of sea surface zonal slope (a proxy for northward velocity) from TOPEX/Poseidon, 1993-2001.

Most of the variance of sea surface zonal slope is associated with westward propagating motions with periods of 50-100 days and zonal wavelengths of 5-13° longitude. Four 1st baroclinic mode Rossby wave dispersion curves are shown. The lower black curve shows the dispersion curve with equal zonal and meridional wavenumbers and zero mean flow. The lower pink curve shows the dispersion curve for a meridional wavenumber of zero and zero mean flow. The upper pair of curves indicate how those curves are modified by a mean westward flow of 11 cm/s (the time-longitude mean of surface currents from Bonjean and Lagerloef (2002) in the region of strongest variability). Since nearly all of the intraseasonal power is bracketed by these dispersion curves, we conclude that these energetic intraseasonal motions are 1st baroclinic mode Rossby waves propagating in the westward flowing North Equatorial Current.

The SST expression of the mesoscale variability

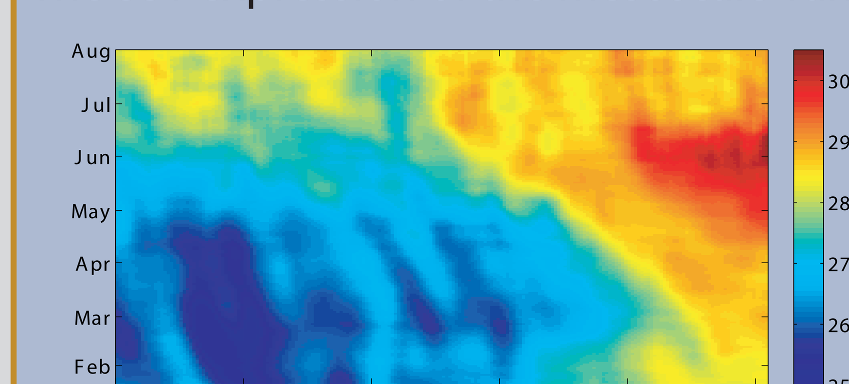

Longitude-time plot of SST along 10°N from the TMI instrument during 1998.

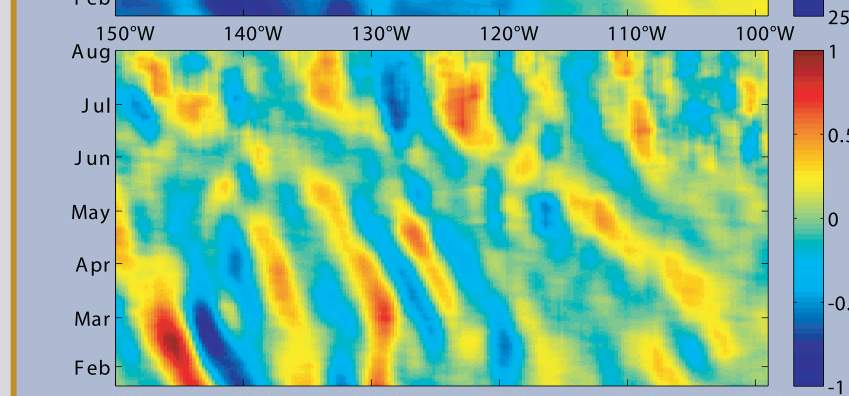

SST along 10°N (as above), high-pass filtered to remove variability at scales larger than 10° longitude.

Most of the variance in SST along 10°N during 1998 (above) is at large spatial and temporal scales (basin and seasonal scales). However, some relatively small variations in SST (O(0.5°C)) can be seen to propagate westward. The SST variations at the 125°W mooring site are clearly visible. These westward propagating SST variations can be seen more clearly when a longitudinal high-pass filter is applied to suppress variability at zonal scales larger than 10° of longitude.

Associated cloud signals

3-week running average visible reflectivity from the GOES-9 satellite (colors).

Contours are warm mesoscale SST anomalies (at 0.2°C intervals).

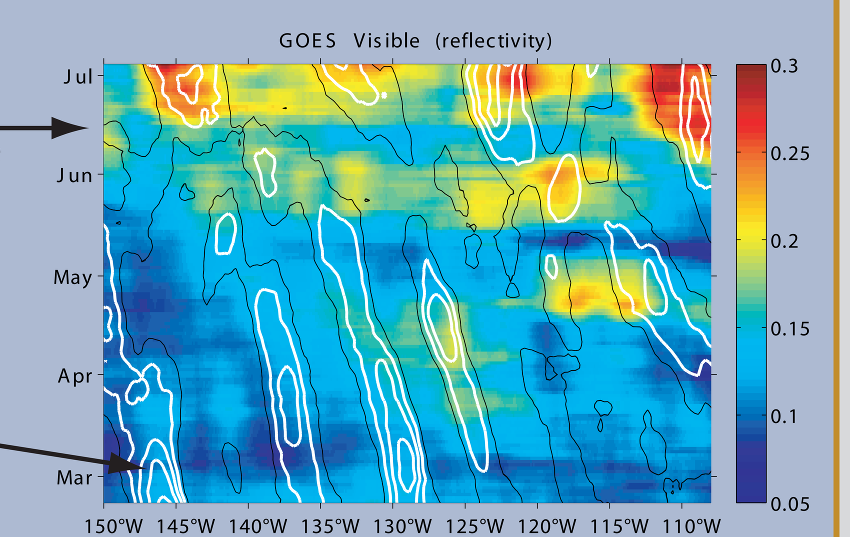

Much of the variability in cloud reflectivity at timescales exceeding a few weeks is associated with zonal scales much larger than the oceanic mesoscale. For example, there are variations in visible reflectivity during May and June that span nearly the full zonal domain of the plot above. When reflectivity is filtered in the same way as SST, a relationship to mesoscale SST fluctuations can be seen more clearly (below).

Zonal 10° high-pass of 3-week running-average visible reflectivity (colors).

Contours are warm mesoscale SST anomalies (at 0.2°C intervals).

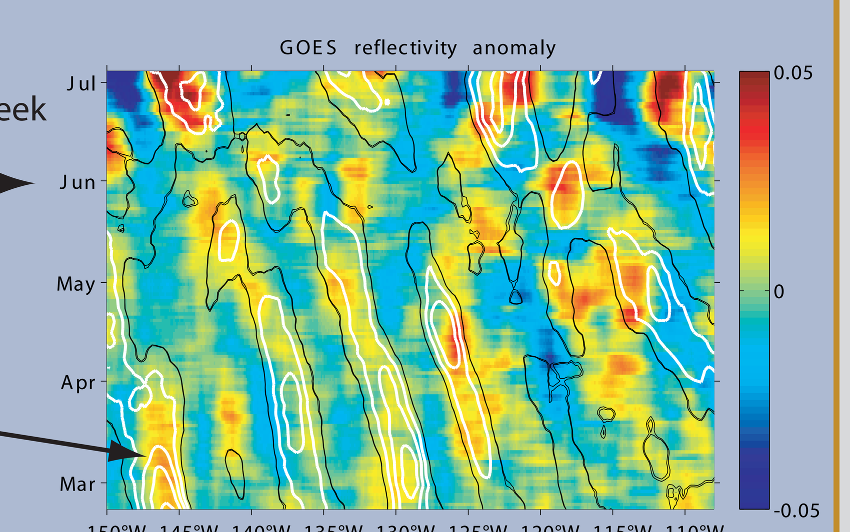

When the cloud reflectivity is high-pass filtered in longitude (10° cutoff), a relationship to the mesoscale SST signal is apparent. The correlation coefficient of the two fields depicted above is about 0.30 (i.e., about 10% of the variance in the filtered reflectivity can be 'explained' by the filtered SST).

Zonal 10° high-pass of $\log_{10}$ of 3-week running-average columnar cloud liquid water (CLW; colors).

A high-pass value of 0.1 indicates a change in CLW of about 26% compared to a zonally smoothed representation of CLW.

(CLW is from both TMI and SSM/I satellite instruments.)

Contours are mesoscale SST anomalies (black is <0, white is >0).

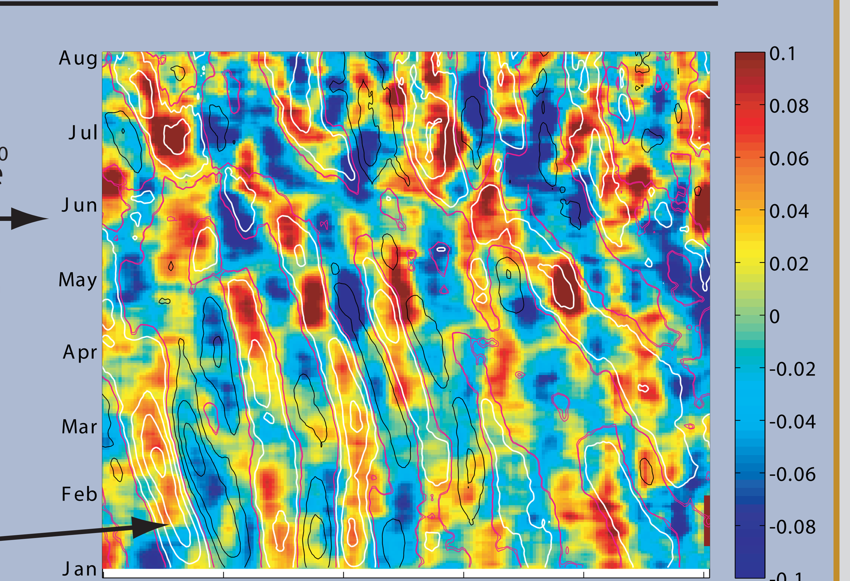

A similar relationship exists between cloud liquid water and oceanic mesocscale SST fluctuations. The $\log_{10}$ of CLW is used because there are larger seasonal variations in CLW as the local conditions shift from the trade-wind regime in Jan-April to ITCZ conditions during the summer. The correlation coefficient of the filtered SST and CLW fields above is also about 0.30.

Conclusion

A more quantitative understanding of the relationship between mesoscale SST fluctuations and cloud properties on 10°N can be obtained by examining the coherence in wavenumber-frequency space. We have done this using satellite SST, CLW, and the ISCCP surface solar radiation product. (Only the coherence of CLW and SST is shown here.) These spectral calculations support the results for the filtered fields to the left.

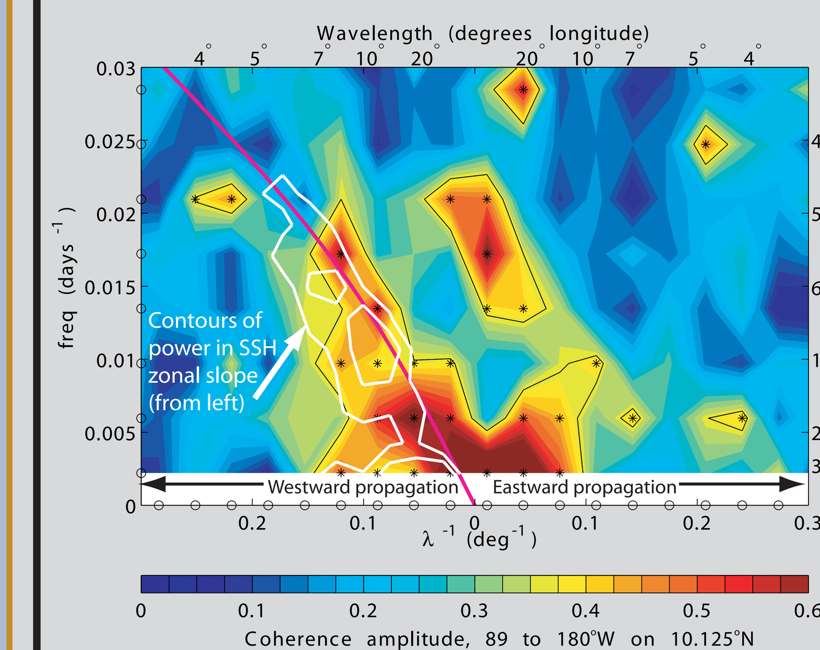

Coherence amplitude of (unfiltered) SST and $\log_{10}$ of CLW. (8 years of data.)

- The white contours show the peak power in the spectrum of sea surface zonal slope (from left), and the pink curve shows the estimated Rossby wave dispersion relation.
- The black contours and asterisks mark points where the coherence is deemed significant at 99% confidence.

The logarithm of CLW is coherent with SST in the oceanic Rossby wave band. Coherence amplitudes at wavelengths of 7-18° longitude and periods of 50-100 days are 0.37-0.60 (statistically significant at 99% confidence), indicating that about 10-35% of the variance in log(CLW) at these wavelengths and periods can be accounted for by SST variations.

The coherence phase (not shown) indicates a nearly in-phase relationship between SST and CLW in the Rossby wave band, with the maximum in CLW shifted westward (downwind) of the maximum in SST by about 1-2° longitude. This is consistent with the relationship between SST and solar radiation observed at the buoy.

While inspection of the filtered CLW and reflectivity fields gives the impression of atmospheric variations co-propagating with the intraseasonal-timescale mesoscale SST anomalies, the coherence of cloud properties with SST is probably best interpreted as a tendency for the SST field to modulate the likelihood and intensity of convection that is embedded within synoptic atmospheric disturbances.

A relationship between mesoscale SST fluctuations and cloud properties has been detected in previous studies in the tropical instability wave region (Deser et al., 1993; Hashizume et al. 2001) and in the mean fields in the Agulhas Return Current southwest of Africa (O'Neill et al., 2005). This study builds on these prior studies, showing a broadband coherence of CLW with SST variations driven by oceanic variability.

Primary references:

C. Deser, J.J. Bates, and S. Wahl. The influence of sea surface temperature gradients on stratiform cloudiness along the equatorial front in the Pacific Ocean. *J. Climate,* 102: 8533-8553, 1993.

J.T. Farrar and R.A. Weller. Intraseasonal variability near 10°N in the eastern tropical Pacific Ocean. *J. Geophys. Res.*, 111, doi: 10.1029/2005JC002989, 2006.

H. Hashizume, S.-P. Xie, T.W. Liu, and K. Takeuchi. Local and remote atmospheric response to tropical instability waves. *J. Geophys. Res.*, 106: 10173-10185, 2001.

L.W. O'Neill, D.B. Chelton, S.K. Esbensen, and F.J. Wentz. High-resolution satellite measurements of the atmospheric boundary layer response to SST variations along the Agulhas Return Current. *J. Climate.*, 18: 2706-2723, 2005.

Acknowledgements: This work was done as part of the U.S. CLIVAR program, with funding from the Cooperative Institute for Climate and Ocean Research and from the PACS program of the NOAA-CPPA. The mooring observations were collected by the WHOI Upper Ocean Processes Group. TMI and SSM/I data were obtained from Remote Sensing Systems. GOES-9 data were obtained from UCAR/JOSS.